TECHNICAL PAPER

The piezoresistive performances of the devices with fullerene-doped MEH-PPV films

Yijie Xia[1] · Luchao Wu[1] · Shuhui Li[2] · ShuaiShuai Du[1] · Zhiyi Wei[2] · Baifan Qian[2] · Gaoyu Zhong[2]

Abstract

A series of devices with the structure of ITO\poly(methoxy-5-(2′-ethylhexyloxy)-1,4-phyenylenevinylene) (MEH-PPV):-fullerene (C60, 0 ∼ 60 wt%)\Al were fabricated and measured. It is found that the device with 20 wt% C60 concentration exhibited an optimized performance for the role of piezoresistive sensing. The piezoresistive coefficient showed $0.12 \sim 0.32$ Pa^{-1} in the pressure range of $0 \sim 396$ kPa. We measured the 20 wt% C60-doped MEH-PPV film using a nanoindentation tester with a flat punch and obtained its Young's modulus at equilibrium state (E_0) to be ∼ 170 MPa. The present work shows that a proper amount of fullerene doped in MEH-PPV film would improve the conductivity of the film, thus leading an enhanced working current density, increasing the current signal for sensing the applied stress, while the necessary elasticity or resilience of the films are maintained. The device performance is optimized through changing the C60 doping concentration to be 20 wt%, approaching a good balance of elasticity and conductivity. Therefore, the device shows a better general performance than the undoped device, exhibiting a better prospect for tactile sensing.

1 Introduction

Polymeric semiconductors are developing rapidly, which have been intensively investigated in the applications of light-emitting diodes, solar cells, organic sensors, etc. These polymers usually have conductive conjugated main chains and insulated saturated side chains. The conjugated main chains make the polymer more conductive, while the side chains separate the main chains, which makes the material easy to be compressed and its conductivity enhanced significantly after the compression. This characteristic of reducing resistance due to the applied stress is called piezoresistance, which can be used to make tactile- or pressure- sensors. At present, the good piezoresistive properties of organic conjugated polymer show prospects in the applications of tactile sensing in robots or pressure sensing in the industry controller (Gong et al. 2014; Kim et al. 2014; Kodzasa et al. 2017; Li et al. 2005; Lipomi et al. 2011; Lötters et al. 1997; Lu and Kim 2014; Schwartz et al. 2013; Someya et al. 2005).

It has been found in previous studies that their conductivity is still low and current density is still little due to the conductivity of many high-purity organic conjugated polymers closer to insulators even after compression. As a result, the absolute value of the change in current density with applied pressure is still insufficient to make the signal in the piezoresistive device relatively large. Despite many conjugated polymers demonstrate good performance in tactile sensors, researchers found that the signal current density is usually too low, while the noise is still serious if the sensed pressure is little. This may be due to the low conductivity of the pure organic conjugated polymers, whose conductive behavior still tend to insulator after compression (Cao et al. 2011; Hou et al. 2017; Li et al. 2019; Mansuroglu and Uzun-Kaymak 2017; Zhong et al. 2009).

To improve the performance of the piezoresistive device, it is necessary to improve the conductivity of the organic conjugated polymer film, i.e. the piezoresistive sensing layer in the device. We have found that the conductivity of materials can be improved if fullerenes are doped in the conjugated polymers in organic light-emitting devices or organic solar cells (Aruna et al. 2015; Smilowitz et al. 1997; Yuan et al. 2005). Therefore, the influence of fullerene doped in poly(methoxy-5-(2′-ethylhexyloxy)-1,4-

✉ Gaoyu Zhong
  gyzhong@fudan.edu.cn

1 School of Mechanical Engineering, University of Shanghai for Science and Technology, Shanghai 200093, China

2 Department of Materials Science, Fudan University, Shanghai 200433, China

phyenylenevinylene) (MEH-PPV) on the piezoresistive performance of the MEH-PPV devices should be investigated.

A fullerene molecule is a spherical 32-hedron composed of 60 carbon atoms. There are large area π bonds on the inside and outside surface. That means electron can move freely along the sp^2 hybrid orbital composed of the carbon atoms. Despite the high conductivity of fullerene, these molecules deform hardly if they are pressed by the low pressure from human hands. Therefore, fullerene cannot be used singly as the tactile sensing material. It can only be doped into the conjugated polymer for improving the performance of piezoresistive devices.

In this work, a pure MEH-PPV piezoresistive device was fabricated and measured. The current density reached ~ 0.05 A/cm^2 at a pressure of 738 kPa, which is similar to our previous study on the piezoresistance of MEH-PPV film (Zhong et al. 2009). Using this device as the control, we fabricated and measured a series of fullerene-doped MEH-PPV piezoresistive devices. The weight percentages of C60 into the mixture in these devices are 0%, 10%, 20%, 40%, and 60%. It was found that the 20 wt% C60-doped MEH-PPV device exhibits optimized performance as the piezoresistive device. It has a higher conductivity compared with the pure MEH-PPV devices, together with better elasticity and softness.

When the pressure ranges from 0 to 396 kPa and the voltage ranges from 0 to 3 V, the piezoresistance coefficient ranges from ~ 0.12 to ~ 0.32 Pa^{-1}. When the pressure reaches 260 kPa and the voltage is 0.2 V, the piezoresistance coefficient reaches the maximum value of 0.32 Pa^{-1}. When the pressure tends to 396 kPa and the voltage is 3 V, the current density of the device tends to saturate, which is ~ 0.5 A/cm^2.

The time-dependent current is also measured with a set containing a function generator and an oscilloscope. The transient characteristics of the devices under different stresses were analyzed. Then we got the construction period of a stable built-in electric field in the device under different stresses, together with the accumulated space charges and the current density reached finally. These data agree with the measured piezoresistive performance of the devices. That means the applied pressure tightened the C60-doped MEH-PPV film, and resulted in a higher current density of the device, together with fewer charges trapped and faster construction of a built-in electric field.

2 Experimental details

Firstly, we purchased the ITO glass commercially as the substrates, with the designed pattern etched on them. Then the substrates were ultrasonically cleaned in acetone, ethanol, and deionized water sequentially, each for 5 min, and then dried in an oven chamber with ~ 1 Pa vacuum at ~ 60 °C.

Secondly, we prepared polymer films as described below. We got the fullerene and MEH-PPV commercially from Sigma-Aldrich Co.Ltd (www.sigmaaldrich.com). Then the fullerene was mixed in the MEH-PPV with the weight concentrations are 0%, 10%, 20%, 40%, and 60%. The mixtures are then dissolved in chloroform (5 mg/ml) and stirred with a magnetic stirrer at ~ 40 °C for 24 h to form completely dissolved solutions with different C60 concentrations (Aruna et al. 2015).

Thirdly, the thin polymer films were prepared using the solutions through spin-coating on the ITO substrates. The rotation rate is 1000 r/min for 60 s. As detailed in reference (Bhardwaj et al. 2020), and agreed with our observation, the doped C60 molecules disperse evenly in the matrix of MEH-PPV. The roughness of the C60 doped MEH-PPV film is very well and make it flat enough to use as tactile sensors (Alegret et al. 2017; Vaez Taghavi and Hirata 2011). Then the formed films were dried in an oven chamber with ~ 1 Pa vacuum for 8 h and the temperature is ~ 25 °C. Then we obtained the ~ 100 nm thick C60-doped MEH-PPV films with different concentrations.

Fourthly, the Al electrodes were deposited on the devices through vacuum evaporation in an OLED fabrication system. The dry C60-doped MEH-PPV films were placed in the chamber, making the vacuum better than 5×10^{-5} Pa. Then the Al source was heated and evaporated, deposited on the polymer films, forming the Al electrode. Then the devices ITO\MEH-PPV: C60 (0%, 10%, 20%, 40%, 60%, 100 nm)\Al were obtained, with the active area is about 3×3 mm^2. The devices were nextly taken out from the chamber and tested the piezoresistive performance directly without any encapsulation. Figure 1 shows the schematic diagram of the measuring set, the molecular structures of C60 and MEH-PPV, together with the device structure.

We measured the piezoresistive characteristics of devices, as detailed following. The Current–Voltage (I–V) curves at different pressures were obtained by changing the pressure or voltage during the test. We used digital force gauge (AIPU, HF-1) to apply different pressures on the device and digital source meter (Keithley, 2400) as the power supply to test the electrical characteristics to obtain the sensitivity, stability, and repeatability under different pressures. We used a clean silicon wafer with the same shape and size as the active area of the devices to cover on the device. The polished surface of the wafer contacted the device directly. We applied pressure at the center of the covering wafer using the gauge stick, which makes the applied pressure uniform and stable, preventing damage to the device. Then, the I–V curves and the Current–Time (I–
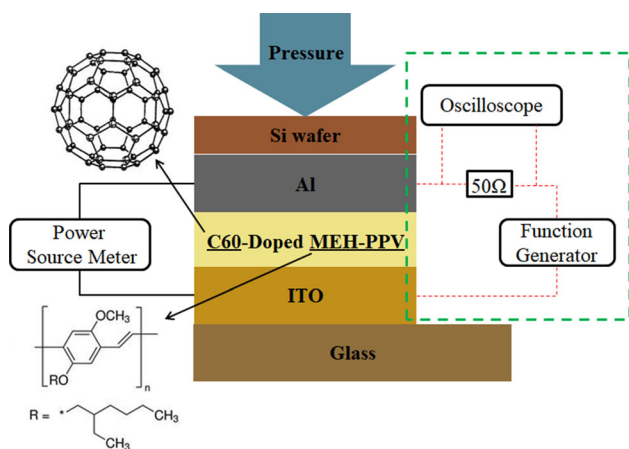
Fig. 1 Schematic diagram of the molecular structure, device structure, and measuring equipment. The right frame shows the oscilloscope, which is used to measure the transient voltage across the 50 Ω resistor

T) curves of the device under constant or square wave voltages were measured under different pressures.

The transient characteristics of the devices were measured under different pressures and high-frequency square wave voltages. The measuring set is shown in the right of Fig. 1. The frequency of the square wave voltage is 5 kHz, and high/low levels are ± 3 V, which is applied on the devices with a function generator (Tektronix-TBS1102). A 50 Ω standard resistor is in series connection with the device, while the voltages across the resistor are measured with an oscilloscope (Tektronix-AFG2021). Based on these time-dependent voltage signals, we analyzed and got three physical parameters varying with stress, including the stable current density, the construction period of the stable built-in electric field in the device, together with the trapped charge amounts during this period.

Finally, the loading–unloading curves of the 20 wt% C60-doped MEH-PPV film were tested with a nanoindenter (UNHT, CSM) by the Oliver and Pharr method (Doerner and Nix 1986; Oliver and Pharr 1992) and fitted with the method described in reference (Zhong et al. 2019a). The sample for the nanoindentation test is prepared through drop-coating to ensure the film thick enough for testing. The film thickness was measured to be 5.526 μm with a surface profilometer (BRUKER DEKTAK150). We used a flat diamond punch with 20 μm diameter as the indenter to prevent the film damage. The maximum load is set to be 0.20 mN. The loading/unloading rate is 0.40 mN/min. The dwell time with the maximum load is 20 s. Young's modulus was calculated through the fitted parameters got from the fitting of the measured load–displacement curve.

3 Results and discussion

The current–voltage (I–V) characteristics of the pristine devices were measured just after taking out from the chamber of the OLED system. The measured I–V curves of the C60-doped MEH-PPV devices with different C60 concentrations of 0%, 10%, 20%, 40%, and 60% by weight are shown in Fig. 2. It is found that the current at the same voltage increases with an increasing concentration of C60. This phenomenon indicates that the conductivity and the working current of the device are enhanced significantly by the doped C60. This phenomenon existed only in the pristine devices, which had not been compressed. If the devices are pressed, no evidence can testify that the conductivity of polymer thin film would increases monotonically with the doped C60 concentration. It may be caused by the lessening of MEH-PPV, which holds the C60 molecules and therefore has a complicated influence on conductivity. These results are coincident with the opinion that the conductivity of organic semiconductors would be improved by doped C60, as reported by Niu et al. (2009) and others (Alegret et al. 2017; Bai et al. 2016; Liao et al. 2013; Niu and Guan 2009). Comparing with the semiconductors of conjugated polymer containing conjugated main chains and saturated side chains, C60 molecules exhibit far more excellent conductance on the outside/inside surface due to the π bonds around the sphere. That means the general conductance of the blended MEH-PPV film would be enhanced by the C60 molecules doped in the organic films.

The I–V curves of the devices with different C60 concentrations were measured under different pressures. The current density–voltage (J–V) curves of the devices with 0% and 10% C60 at different pressures are shown in Fig. 3 and that of the devices with 20%, 40%, and 60% C60 are shown in Fig. 4. It can be seen that the current density
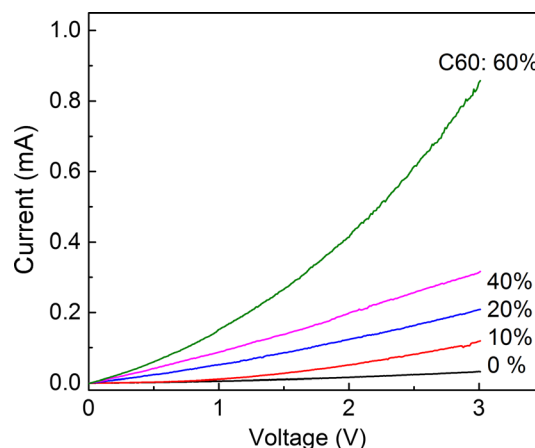

Fig. 2 The I–V curves of the pristine devices with different C60 concentrations

increases with increasing pressure. When the C60 concentration is 0%, its current density will also increase with the increase of pressure, but its current is less, and its I–V curve bends more seriously, which means the I–V curve exhibits a stronger diode characteristic, i.e. its conductive mechanism tends to tunnel effect rather than Ohm's Law.

When the C60 concentration is 0% and the pressure is 738 kPa, the current density has not yet reached saturation, and the current density is about 0.05 A/cm^2 at 3 V. When the C60 concentration is 10%, the current density at the same pressure has increased significantly compared to the 0% concentration. At a pressure of 353 kPa, the current density has reached saturation, 0.11 A/cm^2 at 3 V. Figure 4 shows the J–V characteristic of the devices of 20%, 40%, and 60% under different pressures. When the C60 concentration is 20%, the current density reaches saturation at 396 kPa, i.e. 0.54 A/cm^2 at 3 V, which is 15 times the current density in the 0% device at the same pressure. When the concentration of C60 is 40%, and the pressure is 407 kPa, the current density reaches saturation, 0.4 A/cm^2 at 3 V. Compared with the device with a 20% C60 concentration, the saturation current density decreased. This may be due to the lessening of the content of MEH-PPV in the polymer film. When pressure is applied, the ability of MEH-PPV to hold and connect the C60 molecules decreases relatively during the deformation of the film, making C60 molecules unable to be connected tightly within the MEH-PPV film, resulting in the resistance increased. Thus the conductivity and the working current density decreases. When the C60 concentration is 60% and the pressure is 163 kPa, the current density reaches saturation, 0.4 A/cm^2 at 3 V. The J–V curve of the device gradually tends to linear, coincident with Ohm's Law, while the device resistance does not change gradually, but it roughly appears two states: on or off. When the pressure is 0 ∼ 98 kPa, the current density is about 0.05 A/cm^2,
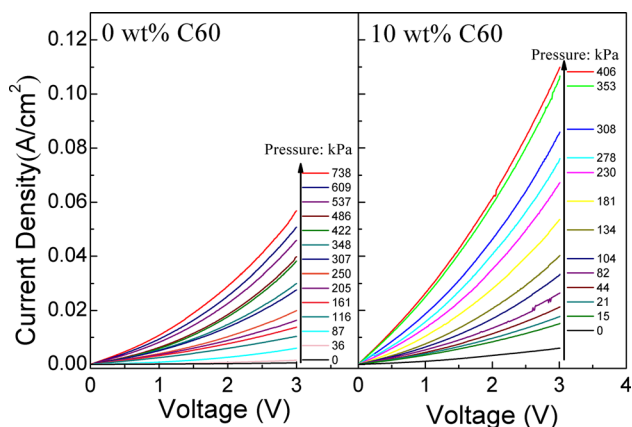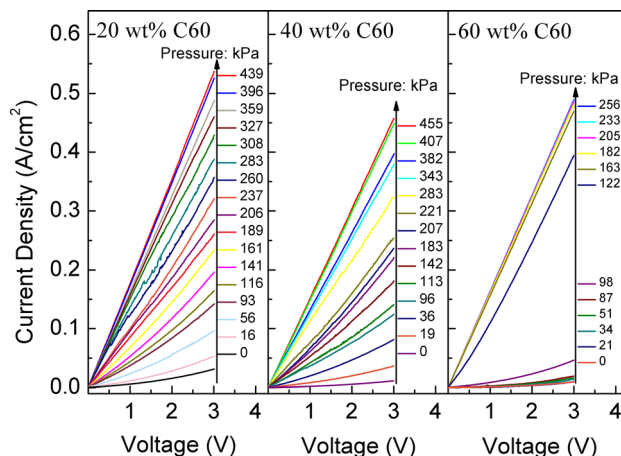

Fig. 4 Current density–voltage (J–V) curves of devices with 20 wt%, 40 wt%, 60 wt% C60-doped MEH-PPV under different pressures

and when the pressure is 122 ∼ 256 kPa, the current density is about 0.45 A/cm^2. In this situation, the content of MEH-PPV is too less and the C60 content is too much, resulting in the film in the device lacks elasticity and the ability of shape recovering, leading to a worse continuity of the current changing with pressure. That means, the device appears open in the circuit if no big enough pressure applies to it, while it tends to be short if a certain pressure applies to it. There are no many medium states between the "on" and "off" state. So the device with high C60 concentration, such as 60%, lacks flexibility.

Summarily, the current density will normally increase with the increasing C60 concentration when it doped in MEH-PPV devices. Among the measured devices with 0%, 10% 20%, 40%, and 60% concentrations, the 20% device showed the best piezoresistive performance. The responsive pressure range is 0 ∼ 396 kPa. So the following detailed analysis focused on the device with 20% C60 concentration. From the data above, we can get the current density varying with stress at different voltages of the device with 20% C60, as shown in Fig. 5. It can be seen that at different voltages, the current density increases with the increasing stress. When the stress varies from 0 to 396 kPa, the current sensitivity of the device is relatively higher. When the pressure approaches 396 kPa and the device at 3 V, the current density is almost saturated at 0.5 A/cm^2. When the pressure is higher than 396 kPa, the current density changes very little. That means the device can work normally in the range of 0 ∼ 396 kPa stress.

Through the I–V curve under different pressures, we got the current amplification factor of the 20% device varying with voltage and pressure, as shown in Fig. 6a. It can be seen that the magnification of current density gradually decreases with the increasing voltage, while at the same voltage, the magnification of current density gradually
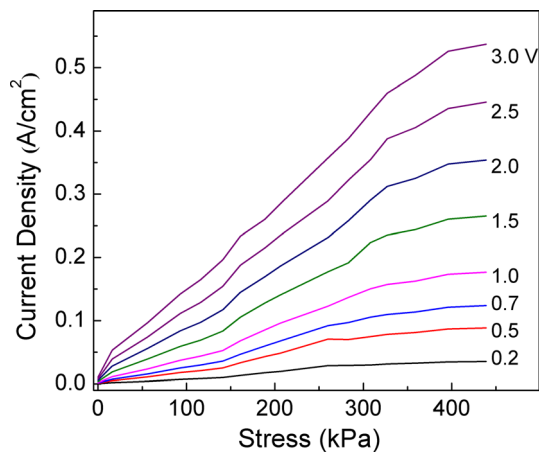

Fig. 3 Current density–voltage (J–V) curves of devices with 0 wt%, 10 wt% C60-doped MEH-PPV under different pressures

Fig. 5 The current density of the device with 20 wt% C60-doped MEH-PPV varying with stress (J–P) under different voltages

increases with the increasing pressure. When the pressure on the device is 0 ~ 56 kPa, the current amplification factor changes more smoothly with the voltage. When the device is applied a voltage higher than 2 V, the current amplification factor changes less with the pressure. As shown in Fig. 6b, the curves of current magnification varying with pressure at different voltages also clearly show the above phenomenon. It can also be seen that when the voltage is 0.2 V and the pressure is 396 kPa, the magnification is higher than 100 times, and the current magnification changes more obviously. Therefore, the device can choose a low working voltage, with low energy consumption and a high current amplification factor, but the working voltage is too low may cause the working current of the device is not very stable. The current instability may be due to the instability of the conductive micropaths involved, the potential carrier tunneling, and the capacitive effect caused by poor contact.
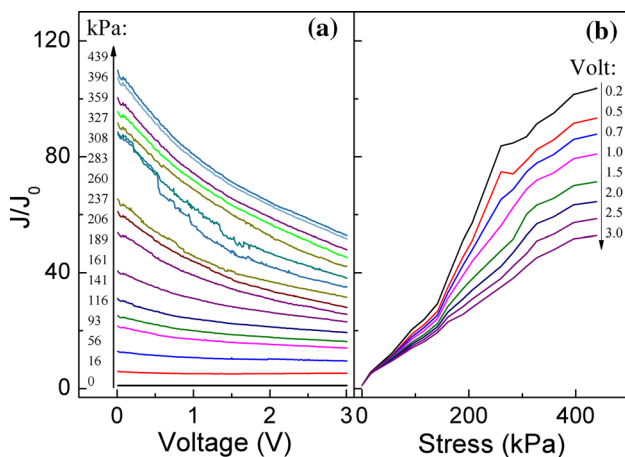
The piezoresistive coefficient can be used to describe the sensitivity of the piezoresistive device (He and Yang 2006). The piezoresistive coefficient is defined as the relative change in conductivity caused by unit pressure (Milne et al. 2010):

$$\pi_l^\rho = \frac{1}{P}\frac{\Delta\sigma}{\sigma_0} = \frac{1}{P}\frac{\Delta J}{J_0},\qquad(1)$$

where σ_0 and $\Delta\sigma$ represent the initial conductivity of the device and its variation, J_0 and ΔJ represent the initial current density and the variation of the device, respectively. Here the J is the current density and P is the external pressure. The greater the piezoresistive coefficient, the higher the sensitivity (He and Yang 2006). Figure 7 shows the variation trend of the piezoresistive coefficient with increasing pressure at different voltages for device with 20% C60 concentration. It can be seen that when the voltage is higher, the piezoresistive coefficient changes less, its trend varying with pressure appears smoother. That means the piezoresistive performance is relatively stable. When the pressure is less than 260 kPa, the piezoresistive coefficient increases gradually; when the pressure is higher than 260 kPa, the piezoresistive coefficient decreases gradually. When the voltage is 0.2 V and the pressure ranges in 0 ~ 396 kPa, the piezoresistive coefficient changes in the range of 0.20 ~ 0.32 Pa^{-1}. The piezoresistive coefficient reaches a maximum of 0.32 Pa^{-1} at 0.2 V and 260 kPa, which is ~ 3000 times of the maximal piezoresistive coefficient (1.1×10^{-4} Pa^{-1}) of MEH-PPV without doped fullerene (Zhong et al. 2009).

We measured the time-dependent current of the 20% device at 3 V voltage under different constant pressures to study the stability of the device, as shown in Fig. 8a. It can be seen that the current is very stable under a fixed
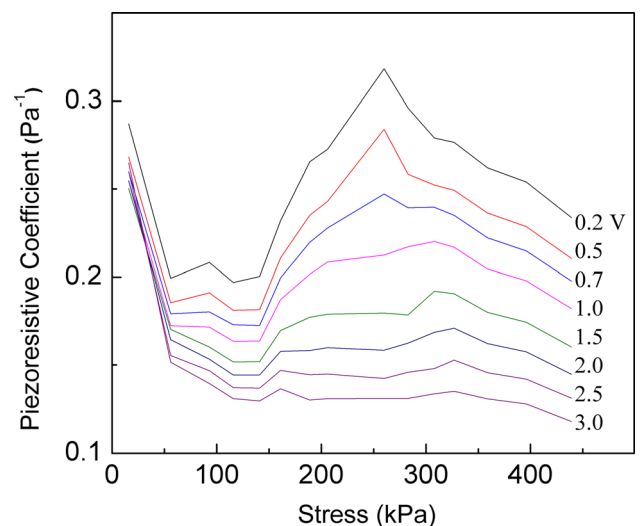

Fig. 6 The current enlargement factors varying with the voltage under different pressures (**a**); the current enlargement factors varying with the pressure under different voltages (**b**)

Fig. 7 The piezoresistive coefficient varying with stress in the range of 0 ~ 396 kPa pressures under different voltages

pressure, maintained at least 60 s, much longer than the response time of the sensor. During this period, the device shows good stability, with relatively very low noise, while the current density increases continuously with the increasing pressure.

We measured current varying with time at different pressures under square wave voltages to study the response of the device to different pressures. As shown in Fig. 8b, the current density of the 20% device under square wave voltages with alternating high and low levels varies with time under different applied pressures. The low and high levels are 0 and 3 V, respectively. Both keeping 10 s in a cycle. The high level is 3 V instead of 0.2 V, mainly to increase the absolute value of the current variation, which is easier to observe. The sharp increase and decrease of the current at 247 kPa in Fig. 8b should be attributed to the capacitance effect, which is due to the appropriate voltage and the intermolecular distance leaded by applied pressures. After charging is complete, the current will drop significantly.

We change the pressure during the low level and remove the original pressure every time before changing the pressure to prevent the current fluctuating too much at a high level. It can be seen that the current density is nearly the same when the device is subjected to the same pressure. The device has good repeatability for loading and unloading, and the response to the electric field is relatively fast. Compared with some other flexible tactile sensors applied in robots, it shows a good prospect for application (Mirza et al. 2016; Sun et al. 2019; Zhong et al. 2019b).

We also measured the time-dependent current of the 20% device at 3 V under alternating pressures of 0 and 352 kPa, as shown in Fig. 9. It can be seen that the current rises rapidly if the device is loaded, while drops quickly
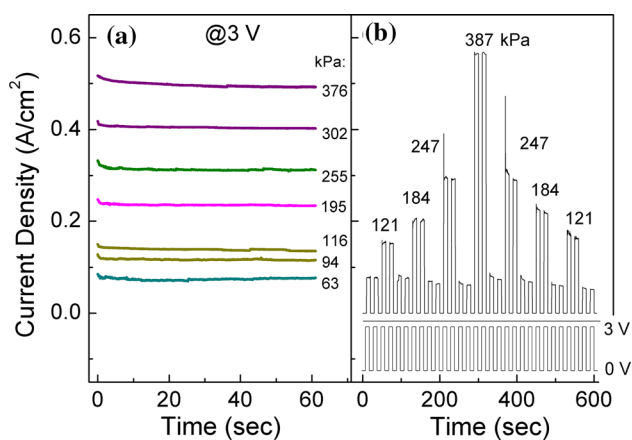
and return to the original value, indicating that the device is very sensitive and responds fast to external pressure. Even the device was pressed by 352 kPa pressure for many times, the current density remained almost the same, 0.5 A/cm^2, indicating that the device has good repeatability and reliability.

To further study the transient characteristics of the device under different pressures, we tested the current signals under different pressures and high-frequency square wave voltages. As shown in Fig. 10, the voltage $V(t)$ across the 50 Ω (R) resistor varied with elapsing time in a half period, and the inset shows the time-dependent voltage across this resistor. It can be seen that the voltage across the 50 Ω resistor increases with the applied pressure when the device reaches a steady state. That means the device current increases with the increasing pressure.

We know that the time (the t in Fig. 10) required for the voltage signal to stabilize is the time required for the device to establish a stable built-in electric field. The integral of current to time during this period is the charge quantity required to establish a stable built-in electric field, which is:

$$Q = \int_0^t \frac{V(t)}{R}\,dt. \tag{2}$$

According to Eq. 2, the charge quantity (Q) required for the device to establish a stable electric field under different pressures can be obtained. Figure 11 shows the time t and charge quantity Q required by the device varies with the applied pressure (P). It can be seen that the time t and charge quantity Q decreases continuously with the increasing pressure. The time (t) required to establish a stable electric field in the device without external pressure
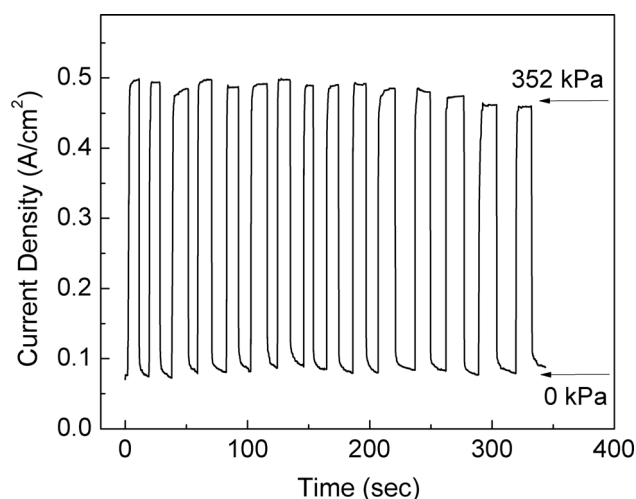

Fig. 8 The time-dependent current density under different pressures at 3 V voltage (**a**); the time-dependent current density varying with the pressure under square-wave voltages applied on the device (**b**). The low and high levels of the voltages are 0 and 3 V, respectively. The duration of the low or high level is 10 s

Fig. 9 The time-dependent current density of the device with 20 wt% C60-doped MEH-PPV under 3 V voltage with alternatively applied pressures of 0 and 352 kPa
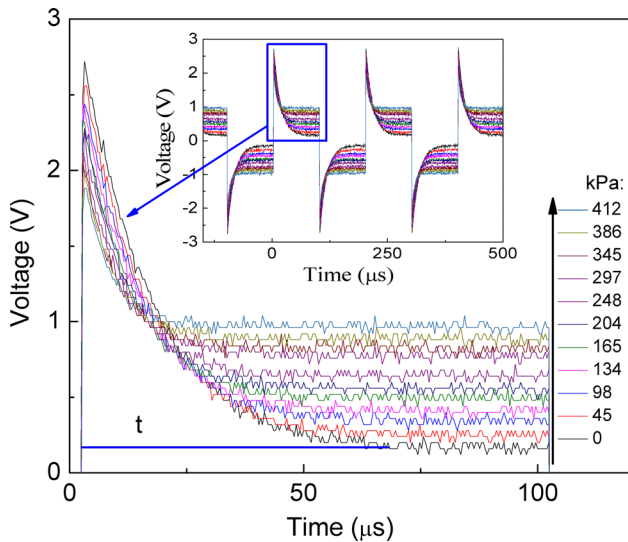
Fig. 10 The time-dependent signal on a 50 Ω resistor of the 20% C60-doped device connected in series into the circuit under varying pressures and square-wave voltages measured with an oscilloscope. The inset shows the voltage varying with elapsing time on the 50 Ω resistor

is 6.0×10^{-5} s, and the required charge (Q) is 7.5×10^{-4} C. This value of Q is complicatedly related to the applied stress, strain, C60 concentration, and device capacitance. If the device is under 386 kPa pressure, the former will be a 1.5×10^{-5} s, and the latter will be 1.4×10^{-4} C. When the pressure exceeds 386 kPa, the time and charge required to establish a stable electric field remain unchanged. This shows that the current through the device is close to saturation and no longer changes significantly as the pressure changes. Figure 12 shows how the current density passing through the device changes with the applied pressure after the device reaches a steady state. It can be seen that when the device reaches a stable state, as the applied pressure increases, the current density through the resistor increases, indicating that the device has a good piezoresistive
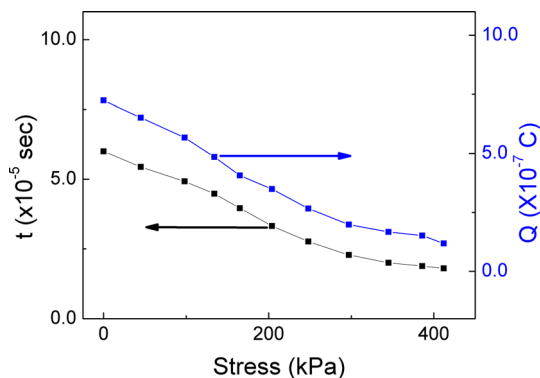
performance. The current density shown in Fig. 12 is lower than the current density in Fig. 5, which may be due to the additional 50 Ω resistors in series in the circuit when we measured the data in Fig. 12.

As shown in Fig. 13a, the doped film has more space between molecules when no stress applied to it. Then it is tightened by the applied stress, as shown in Fig. 13b. The distance between the molecules decreases as the applied pressure increases, the electrons are more likely to jump between the molecules, and the time required to pass through the electric field in the device is thus reduced, then the carrier mobility improved. The applied pressure narrowed the space between molecules, causing the internal electric field increases at the same voltage, making some trapped carriers easier to escape from the trap and be pulled out to participate in conduction, then the carrier density increased. That means the doped C60 improves the carrier density and mobility, improving the conductivity of the device in many aspects. Thus the current signal enhanced and the noise reduced, improving the piezoresistive performances of this kind of device. At the same time, the carrier trap decreases, and the corresponding trapped carriers also decrease. That means the pressure will result in the charge quantity required to establish a stable built-in electric field decreases accordingly. The involved piezoresistive mechanism and conductive mechanism are detailed in reference (Dai et al. 2013; Pope and Swenberg 1999).

Not only the high conductivity of C60 will improve the doped film conductance, but also the energy level alignment of C60 will enhance the electron injection from the Al cathode to the C60 doped in the MEH-PPV film, as shown in Fig. 14. Because the LUMO of C60 is 4.4 eV, no energy barrier exists when an electron injects from the Al electrode (4.3 eV Fermi level) to C60 doped in MEH-PPV.
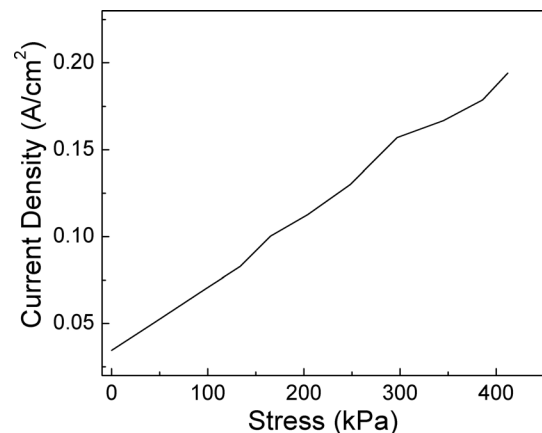

Fig. 11 The required quantity of electric charge and the time needed in the device to establish a stable electric field varying with the applied pressures

Fig. 12 The current density varying with pressures of the stable-achieved 20% C60-doped devices
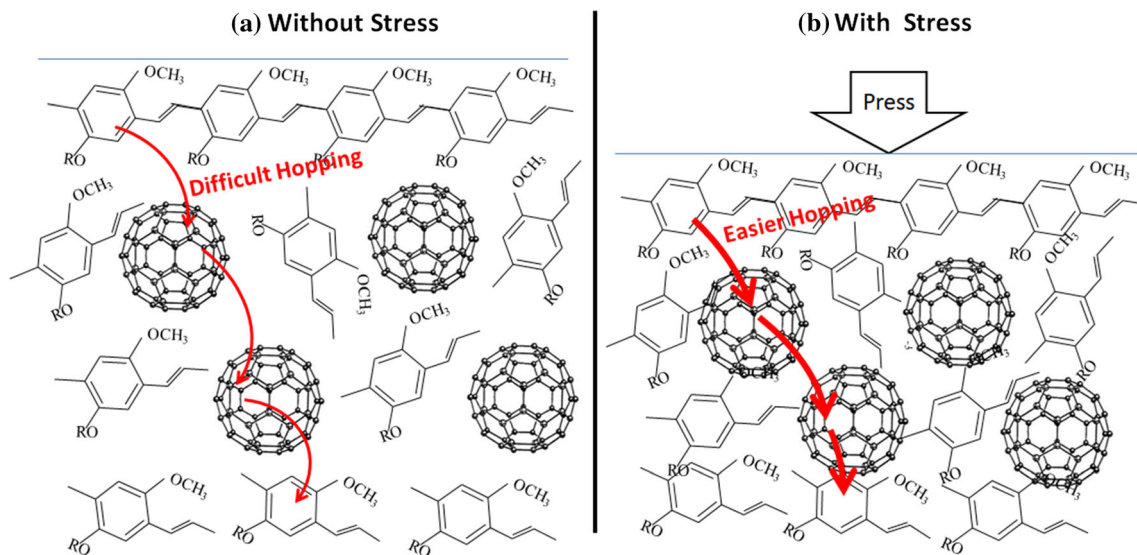
Fig. 13 **a** Schematic diagram of a uniform dispersive C60 doped MEH-PPV film, which is loose because no stress applied to it; **b** Schematic diagram of a uniform dispersive C60 doped MEH-PPV film, which is tightened by the applied stress

But the energy barrier is 1.2 eV when electrons inject directly onto the LUMO of pure MEH-PPV film.

We tested the loading–unloading curves of this doped material with a nanoindenter to study the mechanical property of the 20% C60-doped MEH-PPV film. As shown in Fig. 15, the red line is the fitted unloading curve. The fitting method is described in our published paper (Zhong et al. 2019a). Here the Young's modulus at equilibrium state, i.e. E_0, is deferent from the usually called E. Different from the E, which getting from the stiffness at the starting of unloading curves, here the E_0 is calculated from the ending of the unloading curve, which is related to the
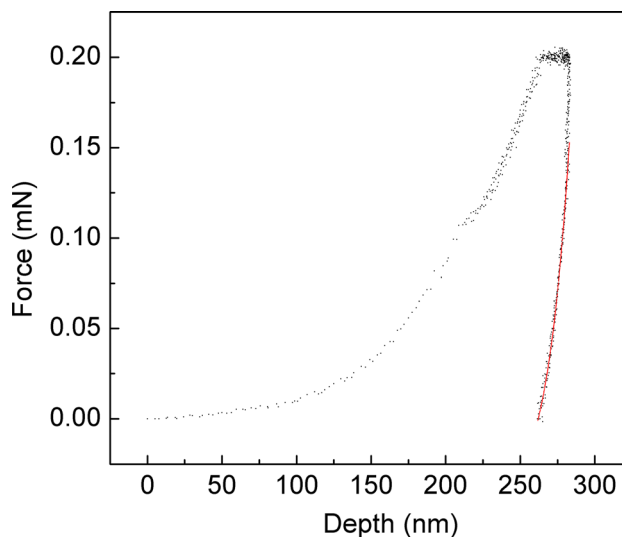

Fig. 15 The loading–unloading curve of 20 wt% C60-doped MEH-PPV thin film, the red line shows the fitted unloading curve
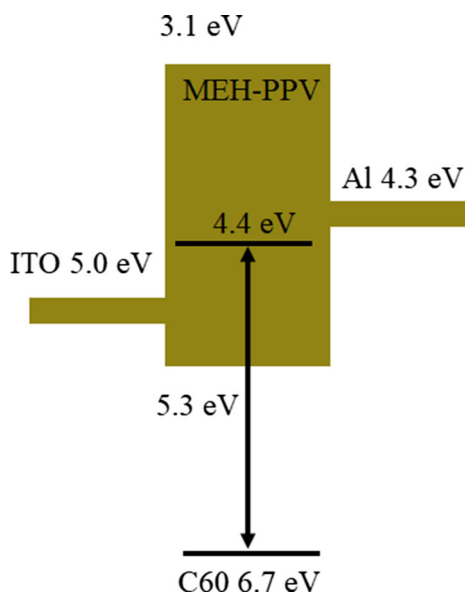
stiffness of the unloading curve under equilibrium state, that means no stress applied on the film at that time. E_0 shows the modulus when a little force touches on the film, while E shows the modulus when a big force applies to the film and begins to release. Generally, the value of E is different from E_0, and E_0 is usually much smaller than E. The fitting results show that Young's modulus (E_0) under the equilibrium state of the MEH-PPV film doped with 20% C60 is $\sim$ 170 MPa, and that of the pure MEH-PPV has been tested to be $\sim$ 70 MPa (Zhong et al. 2019a). That means the added 20% rigid C60 increases Young's modulus at equilibrium state (E_0) from $\sim$ 70 to $\sim$ 170 MPa. The doping of rigid C60 reduces the relative content of

Fig. 14 The energy level alignment of C60-doped MEH-PPV devices

MEH-PPV in the film, not only increases Young's modulus (similar to stiffness) but also decreases the elasticity and the shape recoverability of the device.

4 Conclusions

We prepared and tested ITO\C60-Doped MEH-PPV\Al devices with fullerene concentrations of 0%, 10%, 20%, 40%, and 60%. The results show that adding fullerene into the MEH-PPV can improve the working current density of the device, and reduce the applied pressure when the device current reaches saturation. It is found that when the fullerene concentration is 20%, the device has the best piezoresistive performance, and its working pressure is roughly in the range of $0 \sim 396$ kPa. At $0.2 \sim 3$ V, the piezoresistive coefficient of the device changes in the range of $0.12 \sim 0.32$ Pa^{-1}. It is deduced that the 20% C60 can keep the device a certain elasticity and shape recoverability, improving the conductivity, and thus get the best comprehensive performance. The transient characteristics of the device under high-frequency square wave voltages further confirmed the above described piezoresistive characteristics. It is found that when the applied pressure gradually increased, the amount of charge and time required for the device to reach a steady-state gradually decreased. The loading–unloading curve measured with nanoindentation confirms that the doped 20% C60 makes Young's modulus at equilibrium state (i.e. E_0) of the film change from ~ 70 to ~ 170 MPa. That means the doping of 20% C60 in MEH-PPV improves its conductivity and simultaneously maintains partial original elasticity, to obtain the optimized general piezoresistive performance. This 20% C60 doped MEH-PPV piezoresistive device has a higher piezoresistive coefficient, and thus leads a better prospect for application.

References

Alegret N, Dominguez-Alfaro A, Salsamendi M, Gomez IJ, Calvo J, Mecerreyes D, Prato M (2017) Effect of the fullerene in the properties of thin PEDOT/C60 films obtained by co-electrodeposition. Inorg Chim Acta 468:239–244

Aruna P, Suresh K, Joseph CM (2015) Effect of fullerene doping on the electrical properties of P3HT/PCBM layers. Mat Sci Semicon Proc 36:7–12

Bai Y, Dong Q, Shao Y, Deng Y, Wang Q, Shen L, Wang D, Wei W, Huang J (2016) Enhancing stability and efficiency of perovskite solar cells with crosslinkable silane-functionalized and doped fullerene. Nat Commun 7(1):12806

Bhardwaj J, Vishnoi R, Sharma GD, Asokan K, Singhal R (2020) Mapping the local structure of fullerene C60 and Cu–C60 nanocomposite thin films by gamma rays irradiation. Mater Chem Phys 252:123192

Cao XA, Jiang ZY, Zhang YQ (2011) Organic thin film structures for high-sensitivity imaging of contact stress distributions. Org Electron 12(2):306–311

Dai W, Zhang B, Kang Y, Chen H, Zhong G, Li Y (2013) The stress-affected carrier injection and transport in organic semiconductor devices. J Phys D Appl Phys 46(38):385103

Doerner MF, Nix WD (1986) A method for interpreting the data from depth-sensing indentation instruments. J Mater Res 1(4):601–609

Gong S, Schwalb W, Wang Y, Chen Y, Tang Y, Si J, Shirinzadeh B, Cheng W (2014) A wearable and highly sensitive pressure sensor with ultrathin gold nanowires. Nat Commun 5(1):1–8

He R, Yang P (2006) Giant piezoresistance effect in silicon nanowires. Nat Nanotechnol 1(1):42–46

Hou W, Gao L, Tian Y, Yan W, Hou Y, Li J, Zhong G (2017) Stress-induced variation of MDMO-PPV film thickness and resistance. Synthetic Met 226:113–118

Kim J, Lee M, Shim HJ, Ghaffari R, Cho HR, Son D, Jung YH, Soh M, Choi C, Jung S, Chu K, Jeon D, Lee S, Kim JH, Choi SH, Hyeon T, Kim D (2014) Stretchable silicon nanoribbon electronics for skin prosthesis. Nat Commun 5(1):1–11

Kodzasa T, Nobeshima D, Kuribara K, Uemura S, Yoshida M (2017) Fabrication and performance of pressure-sensing device consisting of electret film and organic semiconductor. Jpn J Appl Phys 56(4S):04CL09

Li Y, Cheng XY, Leung MY, Tsang J, Yuen TXM, MCW. (2005) A flexible strain sensor from polypyrrole-coated fabrics. Synthetic Met 155(1):89–94

Li J, Li J, Hou Y, Hou Y, Wang Y, Wang Y, Ye F, Ye F, Zhong G, Zhong G (2019) The piezoresistance of a device with polyphenylenevinylene derivative PSS-PPV film. Microsyst Technol 25(2):423–430

Liao S, Jhuo H, Cheng Y, Chen S (2013) Fullerene derivative-doped zinc oxide nanofilm as the cathode of inverted polymer solar cells with low-bandgap polymer (PTB7-Th) for high performance. Adv Mater 25(34):4766–4771

Lipomi DJ, Vosgueritchian M, Tee BC, Hellstrom SL, Lee JA, Fox CH, Bao Z (2011) Skin-like pressure and strain sensors based on transparent elastic films of carbon nanotubes. Nat Nanotechnol 6(12):788–792

Lötters JC, Olthuis W, Veltink PH, Bergveld P (1997) The mechanical properties of the rubber elastic polymer polydimethylsiloxane for sensor applications. J Micromech Microeng 7(3):145–147

Lu N, Kim D (2014) Flexible and stretchable electronics paving the way for soft robotics. Soft Robot 1(1):53–62

Mansuroglu D, Uzun-Kaymak IU (2017) Enhancement of electrical conductivity of plasma polymerized fluorene-type thin film under iodine and chlorine dopants. Thin Solid Films 636:773–778

Milne JS, Rowe ACH, Arscott S, Renner C (2010) Giant Piezoresistance Effects in Silicon Nanowires and Microwires. PHYS REV LETT 105(22):226802

Mirza F, Sahasrabuddhe RR, Baptist JR, Wijesundara MBJ, Lee WH, Popa DO (2016) Piezoresistive pressure sensor array for robotic skin. In: D. Popa and M. Wijesundara (Eds) Proceedings of SPIE, pp. 98590K-98590K-12, SPIE, Baltimore, Maryland, United States

Niu L, Guan Y (2009) Fullerene-doped hole transport NPB layer in organic light-emitting devices. Acta Phys Sin-Ch Ed 58(7):4931–4935

Oliver WC, Pharr GM (1992) An improved technique for determining hardness and elastic modulus using load and displacement sensing indentation experiments. J Mater Res 7(6):1564–1583

Pope M, Swenberg CE (1999) Electronic processes in organic crystals and polymers. Oxford University Press, Oxford

Schwartz G, Tee BCK, Mei J, Appleton AL, Kim DH, Wang H, Bao Z (2013) Flexible polymer transistors with high pressure sensitivity for application in electronic skin and health monitoring. Nat Commun 4(1):1–8

Smilowitz L, McBranch D, Klimov V, Grigorova M, Robinson JM, Weyer BJ, Koskelo A, Mattes BR, Wang H, Wudl F (1997) Fullerene doped glasses as solid state optical limiters. Synthetic Met 84(1–3):931–932

Someya T, Kato Y, Sekitani T, Iba S, Noguchi Y, Murase Y, Kawaguchi H, Sakurai T (2005) Conformable, flexible, large-area networks of pressure and thermal sensors with organic transistor active matrixes. Proc Natl Acad Sci 102(35):12321–12325

Sun X, Sun J, Li T, Zheng S, Wang C, Tan W, Zhang J, Liu C, Ma T, Qi Z, Liu C, Xue N (2019) Flexible tactile electronic skin sensor with 3D force detection based on porous CNTs/PDMS nanocomposites. Nano-Micro Lett 11(1):1–14

Vaez TH, Hirata A (2011) Deposition of amorphous carbon films from C60 fullerene sublimated in electron beam excited plasma. Diam Relat Mater 20(7):1036–1041

Yuan Y, Grozea D, Lu ZH (2005) Fullerene-doped hole transport molecular films for organic light-emitting diodes. Appl Phys Lett 86(14):143509

Zhong GY, Zhang YQ, Cao XA (2009) Conjugated polymer films for piezoresistive stress sensing. IEEE Electr Device L 30(11):1137–1139

Zhong GY, Yan WQ, Li J, Tian YM (2019a) Determining Young's modulus of MEH-PPV film by fitting the unloading curve. Microsyst Technol 25(4):1467–1474

Zhong W, Ding X, Li W, Shen C, Yadav A, Chen Y, Bao M, Jiang H, Wang D (2019b) Facile fabrication of conductive graphene/polyurethane foam composite and its application on flexible piezo-resistive sensors. Polymers-Basel 11(8):1289